Impact of Structural Variability on Robust Flutter Optimization

53rd AIAA/ASME/ASCE/AHS/ASC Structures, Structural Dynamics and Materials Conference
20th AI
23 - 26 April 2012, Honolulu, Hawaii

AIAA 2012-1709

Impact of Structural Variability on Robust Flutter Optimization

S. Marques*

School of Mechanical and Aerospace Engineering, Queen's University Belfast, Belfast

K. J. Badcock†

School of Engineering, University of Liverpool, Liverpool, UK, L69 3GH

I. NOMENCLATURE

Symbols

A	Jacobian matrix
f	aerodynamic forces
$\mathbf{p}$	eigenvector
$\mathbf{R}$	Residual vector of the fluid and/or structural model
S	Schur complement matrix
$\mathbf{w}$	vector of fluid and/or structural unknowns

Greek

α	polynomial chaos coefficients
λ	eigenvalue
γ	Bifurcation parameter (altitude)
μ	mean
ϕ	normal mode shape
θ	Vector containing the uncertain structural parameters
ω	normal mode frequency
Ψ	basis function
σ	standard deviation
θ	optimization design variables
ξ	structural model variables

Subscripts or superscripts

f	fluid model
s	structural model
0	equilibrium

II. Introduction

CURRENT standard aeroelastic and flutter analysis relies on deterministic calculations, where all required properties and parameters are defined by specific values. Wing structural optimization in the presence

*Lecturer, MAIAA, corresponding author; Tel.: +44(0)28 9097 4185; Email: s.marques@qub.ac.uk
†Professor, SMAIAA

of aeroelastic instabilities in the transonic regime has been attempted despite the high computational cost required by nonlinear aerodynamics. Janardhan and Grandhi maximized the store-induced flutter speed by increasing the difference between the first two natural frequencies,[1] Marques *et al.*[2] performed structural optimization for uncertainty quantification on wings and full aircraft configurations.

Since there is an intrinsic variability in many of the components that influence aeroelastic behaviour, there has been a recent trend to apply non-deterministic methods as discussed by Pettit.[3] Developments in computational aeroelasticity[4] enabled researchers to perform uncertainty quantification due to structural variability for flutter in transonic regimes.[2] Further studies also showed the impact of tip store c.g. location on the nature and development of the flutter instability boundary.[5] Changes in tip store properties such as c.g. location and mass impact on the location of the wing's flexural axis, natural frequencies and mode shapes. It was also shown how the mode shapes can have be a dominant factor on aeroelastic damping.

A recent study incorporated stochastic outputs representing structural variability into a flutter optimization framework.[6] This allowed the use of stochastic quantities such as means or standard deviations to be use as objective function in order to produce robust or reliable optimums. It was concluded that for the set of design variables used, the mean and standard deviations converged to very similar optimum points. This paper is a continuation of this effort by examining in more detail the structural characteristics that influence each of the two stochastic outputs. A systematic study of the Goland wing will be presented, assessing the impact of structural properties and components on the stochastic optimization results. Results applying the same techniques for a realistic transport wing are also presented and discussed.

III. Aeroelastic Stability Formulation

The semi-discrete form of the coupled CFD-FEM system is written as

$$\frac{d\mathbf{w}}{dt} = \mathbf{R}(\mathbf{w}, \gamma) \tag{1}$$

where

$$\mathbf{w} = [\mathbf{w}_f, \mathbf{w}_s]^T \tag{2}$$

is a vector containing the fluid unknowns ($\mathbf{w}_f$) and the structural unknowns ($\mathbf{w}_s$), and

$$\mathbf{R} = [\mathbf{R}_f, \mathbf{R}_s]^T \tag{3}$$

is a vector containing the fluid residual ($\mathbf{R}_f$) and the structural residual ($\mathbf{R}_s$). In this paper, the fluid model is given by the Euler equations, whereas the structural model is defined by the following scalar equations

$$\frac{d^2\xi_i}{dt^2} + D_i\frac{d\xi_i}{dt} + \omega_i^2\xi_i = \frac{\rho_\infty}{\rho_w}\phi_i^T f_s \tag{4}$$

where ξ_i are the generalized coordinates, ϕ_i represents the mode shapes extracted from the finite element model, D_i are the damping coefficients, f_s is the vector of aerodynamic forces at the structural grid points and ρ_∞/ρ_w is the density ratio between air and the wing;

As described above, the residual depends on a parameter γ (altitude in this paper) which is independent of $\mathbf{w}$. An equilibrium $\mathbf{w}_0$ of this system satisfies $\mathbf{R}(\mathbf{w}_0, \gamma) = \mathbf{0}$.

The linear stability of equilibria of equation (1) is determined by eigenvalues of the Jacobian matrix $A = \partial\mathbf{R}/\partial\mathbf{w}$. The calculation of the Jacobian A is most conveniently done by partitioning the matrix as:

$$A = \begin{bmatrix} \frac{\partial \mathbf{R}_f}{\partial \mathbf{w}_f} & \frac{\partial \mathbf{R}_f}{\partial \mathbf{w}_s} \\ \frac{\partial \mathbf{R}_s}{\partial \mathbf{w}_f} & \frac{\partial \mathbf{R}_s}{\partial \mathbf{w}_s} \end{bmatrix} = \begin{bmatrix} A_{ff} & A_{fs} \\ A_{sf} & A_{ss} \end{bmatrix}. \tag{5}$$

Details of the implementation of the Euler and structural equations and Jacobian calculation can be found in references[7] and.[8] In the current work, and as is conventional in aircraft aeroelasticity, the structure is modeled by a small number of modes, therefore the number of the fluid unknowns is far higher than the structural unknowns. This means that the Jacobian matrix has a large, but sparse, block A_{ff} surrounded by thin strips for A_{fs} and A_{sf}.

The coupled system eigenvalue problem $A\mathbf{p} = \lambda\mathbf{p}$, where $\mathbf{p}$ and λ are the complex eigenvector and eigenvalue respectively, is solved using the Schur complement based on A_{ff}. Assuming λ is not an eigenvalue of A_{ff}, the eigenvalue satisfies the nonlinear eigenvalue problem:[9]

$$S(\lambda)\mathbf{p}_s = \lambda\mathbf{p}_s \tag{6}$$

where $S(\lambda) = A_{ss} - A_{sf}(A_{ff} - \lambda I)^{-1}A_{fs}$. Details of the implementation of the eigenvalue solver can be found in reference.[4] This method has successfully been applied to the study of the influence of structural variability on aeroelastic stability in the transonic regime using several non-deterministic techniques.[2,5]

IV. Stochastic Modeling

The approach used in this paper is based on a non-intrusive polynomial chaos (NIPC) method. NIPC have been used successfully in different aeroelastic problems,[10–12] where sampled points from the parameter space are used to reconstruct a "polynomial expansion". The basic equation for the truncated polynomial chaos expansion (PCE) can be expressed as:

$$u(\mathbf{x}) = \sum_{i=1}^{n_b} \alpha_i \Psi_i(\xi(\mathbf{x})) \tag{7}$$

where $\mathbf{x}$ represents the set of uncertain variables, u is the response of interest, α_i are polynomial coefficients, the basis functions Ψ_i represent orthogonal polynomials based on the random variables ξ. The random variable ξ is obtained by an appropriate transformation of the original variables $\mathbf{x}$. The orthogonal polynomials used to define the basis function, Ψ, depend on type of the random variables, for example in the case of normal distributions, Hermite polynomials are typically used, whereas for uniformly distributed inputs Legendre polynomials are chosen. For a specified order of the polynomial, P, a set of $P+1$ vectors ξ_i for $i = 0, 1, 2, ..., P$ are used in the approximation. Hosder *et al.*[12] suggest latin hypercube sampling to estimate the expansion coefficients α_i by solving the following linear system:

$$\begin{bmatrix} \Psi_0(\xi_0) & \Psi_1(\xi_0) & \cdots & \Psi_P(\xi_0) \\ \Psi_0(\xi_1) & \Psi_1(\xi_1) & \cdots & \Psi_P(\xi_1) \\ \vdots & \vdots & \ddots & \vdots \\ \Psi_0(\xi_P) & \Psi_1(\xi_P) & \cdots & \Psi_P(\xi_P) \end{bmatrix} \begin{bmatrix} \alpha_0 \\ \alpha_1 \\ \vdots \\ \alpha_P \end{bmatrix} = \begin{bmatrix} u_0(\mathbf{x}) \\ u_1(\mathbf{x}) \\ \vdots \\ u_P(\mathbf{x}) \end{bmatrix} \tag{8}$$

With the regression model built, Monte-Carlo analysis can be used with the regression model to obtain the statistic quantities of interest, usually $10^5 - 10^6$ samples are enough to obtain consistent outputs.

V. Optimization Framework

The aim of this paper is to investigate the possibility of minimizing the impact of variability on the structure flutter response, ie the objective is to find a set of parameters that maximize the robustness of the structure with respect to external stores variability. The formulation of this robust design problem makes use of the mean and standard deviation obtained by statistical methods, and can be expressed as:[13]

find

$$\theta \in \Re^n \tag{9}$$

to minimize

$$[\mu(\lambda(\theta, \mathbf{x})),\ \sigma(\lambda(\theta, \mathbf{x}))] \tag{10}$$

subject to

$$\underline{\theta} < \theta < \overline{\theta} \tag{11}$$

where $\mathbf{x}$ represents aleatory structural properties and θ are the parameters to be optimized. This robust optimization formulation resembles a multi-point optimization problem, where two outputs are required to be minimized. A common approach to solve such problems is to combine the mean and standard deviations

in the form of a weighted sum:

$$\begin{aligned} &\text{minimize} \\ &\qquad f(\mu,\ \sigma) \\ &\text{subject to} \\ &\qquad \underline{\theta} < \theta < \overline{\theta} \\ &\text{with} \\ &\qquad f(\mu,\ \sigma) = \beta \left[\frac{\mu(\lambda(\theta,\mathbf{x}))}{\mu^*}\right] + (1-\beta)\left[\frac{\sigma(\lambda(\theta,\mathbf{x}))}{\sigma^*}\right] \end{aligned} \tag{12}$$

the mean and standard deviations are non-dimensionalize by μ^* and σ^*, corresponding to the mean and standard deviations of the original structure, respectively. The optimization problem can be solved by many different methods. In this work the **NLOPT** toolbox[14] provides an adequate range of algorithms suitable to solve such problems, including gradient and gradient free methods. Although typically gradient methods converge to a local minimum faster that gradient free methods, the extra computational cost of computing gradients with respect to stochastic outputs was seen as impractical. It was therefore decided to used a derivative free algorithm known as **COBYLA**,[15] which constructs linear polynomial approximations to the objective and constraint functions by interpolation at the vertices of simplices. The **NLOPT** toolbox can be set up in many different environments: Octave, Python, C++, etc. In this work an optimization framework was built in Python. **NLOPT** requires the user to supply the objective function, which in this case corresponds to the output of the NIPC approach; the sampling process for the NIPC is done in parallel with Python scripts driving the required aeroelastic analysis.

VI. Results

A. Goland Wing+

The Goland wing, shown in figure 1(a), has a chord of 1.83m and a span of 6.1m. It is a rectangular cantilevered wing with a 4% thick parabolic section. The structural model follows the description given in reference.[16] The CFD grid is block structured and uses an O-O topology. The fine grid has 250 thousand points and a coarse level was extracted from this grid, which has 40 thousand points. Grid refinement results reported previously in reference[4] showed that the coarse grid gives accurate aeroelastic damping predictions. Four mode shapes were retained for the aeroelastic simulation, the first and second bending and torsion modes. The nominal conditions of this case correspond to M=0.90 and $\alpha = 0°$, this is characterized by a strong shock-wave towards the trailing edge as illustrated by the CFD solution in figure 1(d).

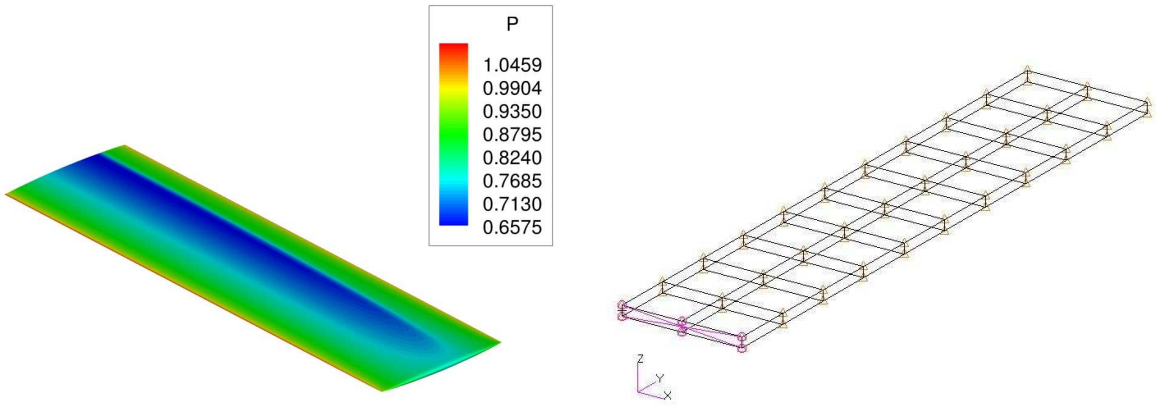

(a) CFD Solution (b) Structural Model

Figure 1. Goland Wing Model

The case considered in this work has a mass added to the wing tip to represent the presence of a tip store. The baseline position is 7.5cm from the wing tip. The store is offset 52.5cm from the elastic axis,

(*ea*), and has a total mass of 328.3kg, which represents 1/10 of the total wing mass (corresponding to the mass of one rib). The baseline location is indicated in figure 1(c). The store c.g. location and mass are considered uncertain; it is the impact of this uncertainty the optimization process aims to minimize. The uncertain parameters are modeled using uniform distributions for the c.g. and mass, described in table 1[a].

Parameter	Mean	Maximum Value	Minimum Values
Store Mass	328.3kg	574.525kg	82.075kg
c.g. location	-0.292c	-0.125c	-0.459c

Table 1. Goland Wing$^+$ optimization parameters

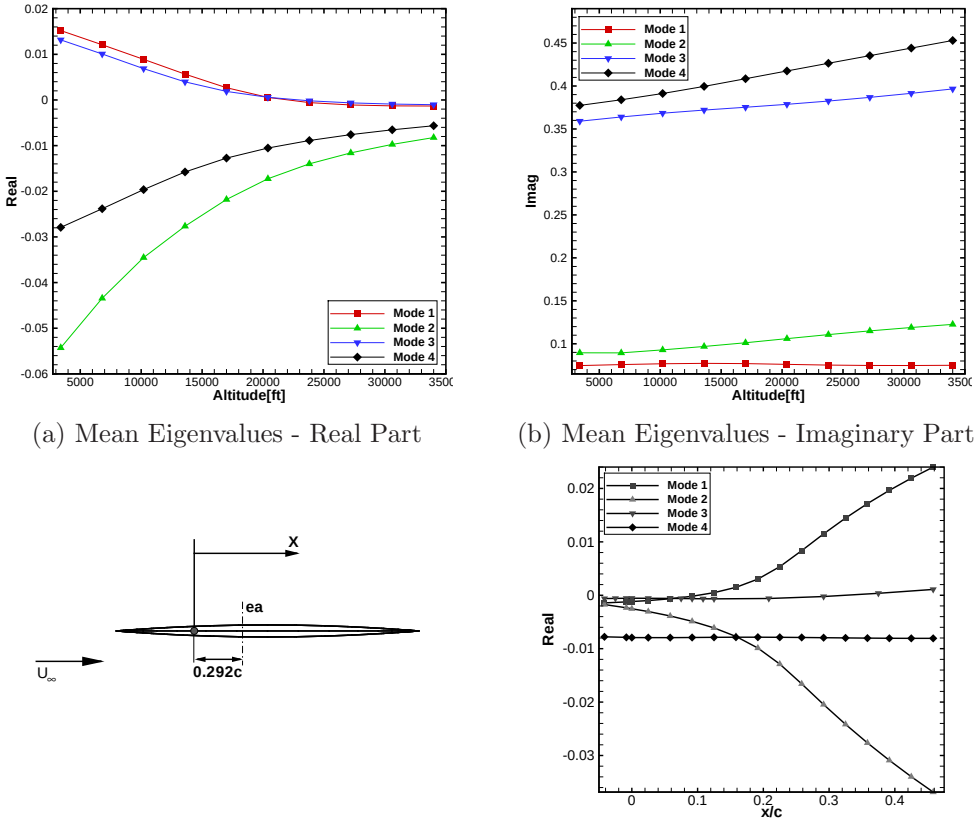

(a) Mean Eigenvalues - Real Part

(b) Mean Eigenvalues - Imaginary Part

(c) Store location

(d) Store location impact on real eigenvalues

Figure 2. Goland Wing - Original Structure

Previous analysis concluded that from the complete structural model, only seven structural properties have a significant influence on the onset of flutter.[6] When using the seven parameters as design variables in the stochastic optimization process together with the uncertain store properties, similar results are obtained regardless of eq.12 using the standard deviation or mean as objective function. It was decided to allow the original 7 parameter to vary along the span, raising the number of design variables to 25. By increasing the design space, different optimums are found when considering only the mean or only the standard deviation as the objective function; the difference is noticeable, but small. The results of the stochastic optimization using 25 design variables is shown in fig. 3-a)-b). Figure 3-c) shows the optimization impact on the real part of the aeroelastic system eigenvalue of mode 1, a reduction of about 5000ft on the flutter altitude is achieved on this mode; the impact of the optimization on reducing the effects of the store variability is illustrated by the histogram in fig.3-d). The results indicate that some properties and their spatial

[a]c.g. location is measured with respect to the original *ea* location

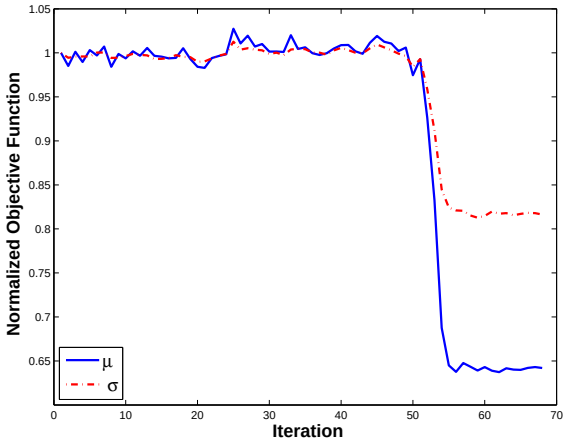

(a) Optimization Convergence - Mean bias

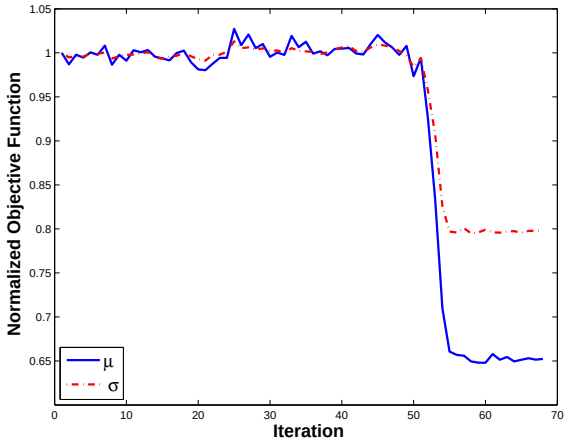

(b) Optimization Convergence - Std. Dev. bias

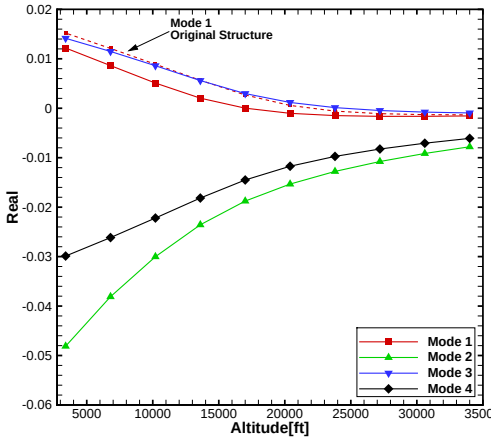

(c) Optimized Mean Real Eigenvalue

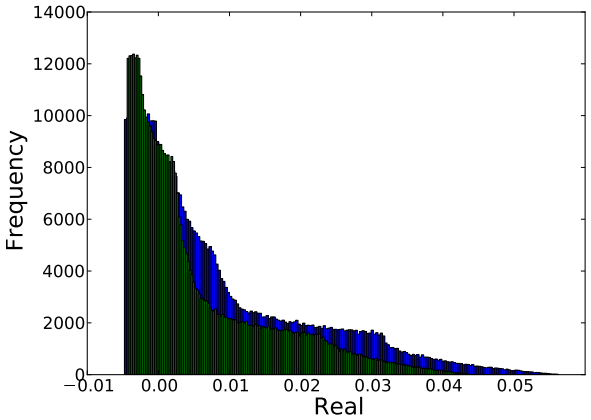

(d) Original (back) and Optimized (front) structure histogram

Figure 3. Optimization at 24000ft, 25 structural design variables

Parameter	Initial Value	Range
Upper Skin thickness	4.715×10^{-3}m	±20%
Lower Skin thickness	4.715×10^{-3}m	±20%
LE Spar thickness	1.825×10^{-3}m	±20%
TE Spar thickness	1.825×10^{-3}m	±20%
LE Spar Cap area	3.865×10^{-3}m^2	±20%
Centre Spar Cap area	1.390×10^{-2}m^2	±20%
TE Spar Cap are	3.865×10^{-3}m^2	±20%

Table 2. Goland Wing$^+$ optimization parameters

location, will have a greater impact on reducing the standard deviation (hence, increasing the optimum robustness), whereas others have a stronger impact on the mean value of the flutter response. The graphs in figure 4 (where lower indexes correspond to properties near the root, higher indexes indicate values towards the tip) show the different optimum values obtained when optimizing the structure with mean or standard deviation bias, respectively. The leading edge spar thickness can change at five locations along the span. In general, when the algorithm minimizes the standard deviation, the structure component thicknesses tend to be maximized. Although the different objective functions give similar results, it worth pointing out that the standard deviation optimization would originate a heavier structure, due to the increase in thicknesses of most components.

B. MDO Wing

The MDO wing is representative of a commercial transport wing. It has a span of 36 metres, the profile is a thick supercritical section designed to operate in the transonic conditions.[17,18] The CFD grid and geometry, as well as the structural model are summarized in fig. 5-a)-b). The structure is modeled as a wing box running down the central portion of the wing. The CFD grid used has 81 thousand points. The eigenvalue formulation used in this paper was applied to the MDO wing in reference.[4,5] In the current work seven modes are retained and the mapped modes which participate in the aeroelastic instability.

Here we consider the case with a freestream Mach number of 0.85 and an angle of attack of 1 degree. The wing Young's modulus for the upper and lower skin panels, and the upper and lower spar caps and skin stringers are used as design variables to optimize, their values is summarized in table 3. As in the previous case, the general objective function is given by eq. 12. An uncertain mass and respective inertial properties is added to the wing tip and is considered to be uncertain; the uncertain tip mass properties are modeled using a uniform distribution as described in table 4. The aeroelastic eigenvalues of the original model were traced with altitude and are shown in fig. 5-c)-d). Stability is lost when modes 1 and 2 become positive at about 4000m. It worth noticing that the mode tracking shows a more rapid increase in mode's 2 real eigenvalue, thus this mode was selected to drive the optimization.

By comparison with the Goland wing test case, the optimization results for the MDO wing are more dramatic. When using the mean value of the real eigenvalue of mode 2 with respect to the uncertain tip mass, the optimization process is quite effective and stability is increase by about 5 times the original value, as illustrated by fig.6-a). However, the standard deviation increases, i.e. the structure becomes more sensitive

Parameter	Initial Value	Range
Upper Skin Panels (E_1)	71×10^9Pa	±25%
Lower Skin Panels (E_2)	71×10^9Pa	±25%
Upper Spar caps / Stringers (E_3)	71×10^9Pa	±25%
Lower Spar caps / Stringers (E_4)	71×10^9Pa	±25%

Table 3. MDO Wing optimization parameters

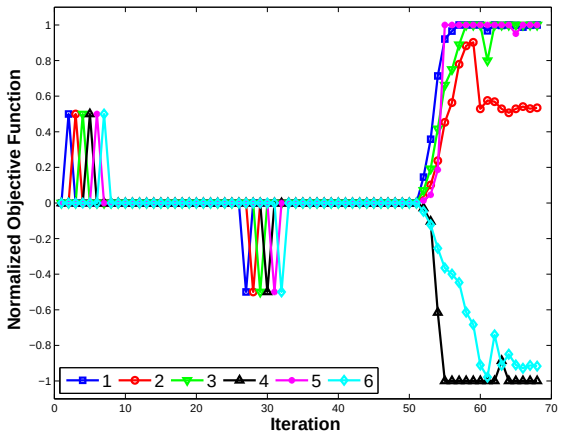

(a) Mean Obj. Function - Upper Skins

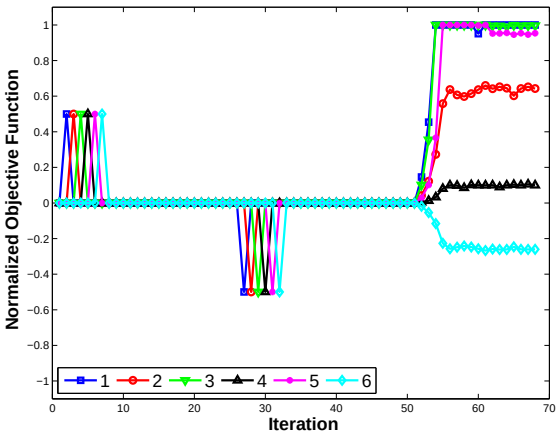

(b) Std. Dev. Obj. Function - Upper Skins

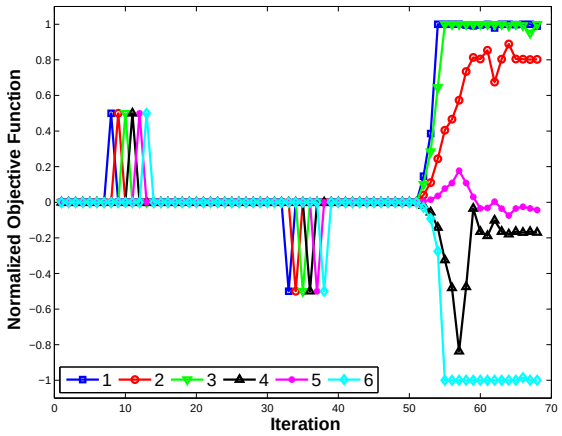

(d) Mean Obj. Function - Lower Skins

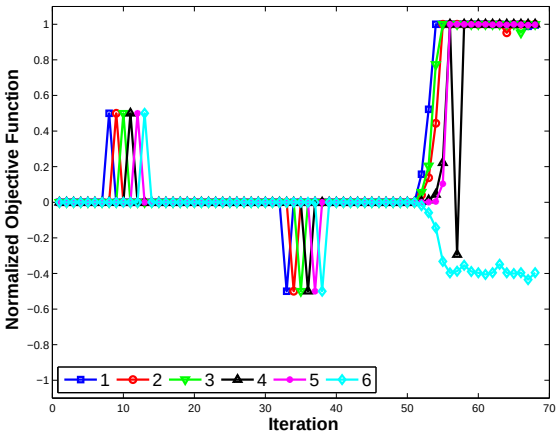

(d) Std. Dev. Obj. Function - Lower Skins

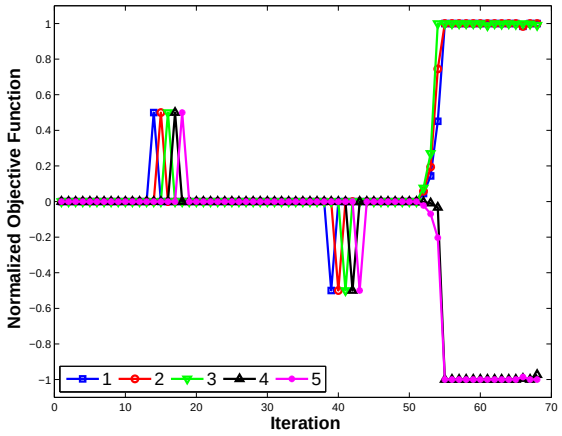

(e) Mean Obj. Function - LE Thickness

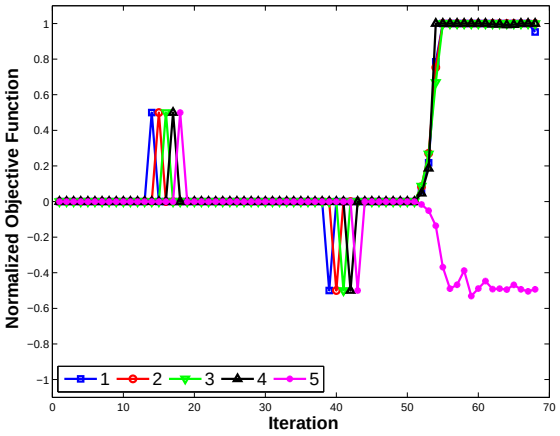

(f) Std. Dev. Obj. Function - Leading Edge Thickness

Figure 4. Goland Wing Optimization

Parameter.	Minimum	Maximum
Tip Mass	0	150kg
Tip Mass I_{yy}, I_{zz}	0	$3300kgm^2$

Table 4. MDO Wing Uncertain Variables Convergence

to variations on the tip inertial properties.

By setting $\beta = 0$ in eq.12, the objective function becomes the standard deviation. Figure 6-c) shows a significant decrease in standard deviation, but the mean value decreases about 2.5 times the original value, significantly less then on the previous case. This also illustrates how sensitive the structure is to changes at the tip. A third optimization problem was set using using $\beta = 0.5$, the optimization impact on the mean and standard deviation are shown in fig.6-e)-f). By combining the two statistical moments an improved compromise was achieved: the mean value of the response was reduced by another factor, i.e. the mean value is now 3.5 times less than the original. Additionally, the standard deviation was still reduced to about 15% of its original value, which is very similar to the result obtained when only using the standard deviation as objective function.

It is interesting to note which parameters are driving the reductions on the objectives functions. The preliminary results presented in this paper, indicate that the stiffness of the upper spar caps and skin stringer have a strong impact on the minimization of the standard deviation, as indicated by fig.6-d)-f).

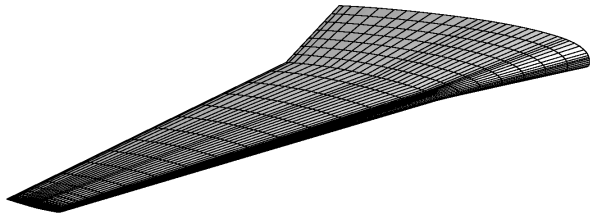

MDO CFD grid

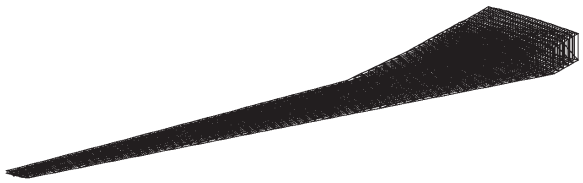

MDO Structural Model

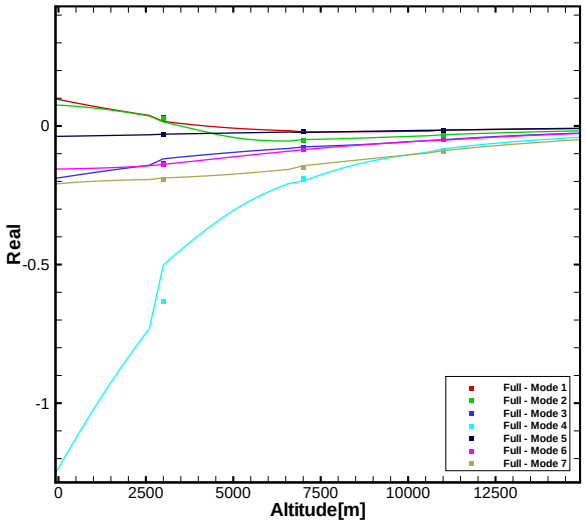

Real Eigenvalue

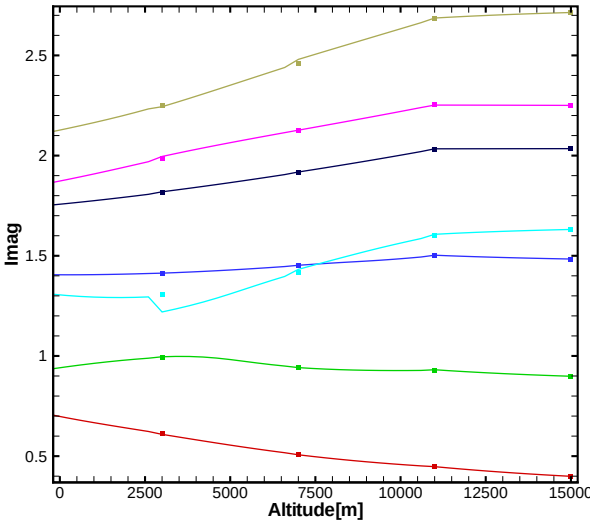

Imaginary Eigenvalue

Figure 5. MDO Wing

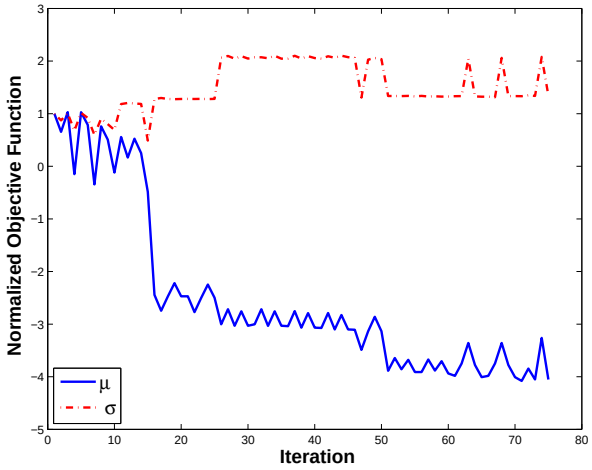

(a) Mean as Objective Function

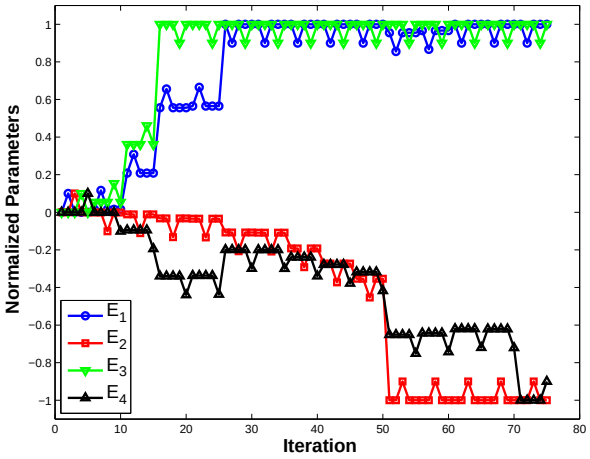

(b) Parameters Convergence

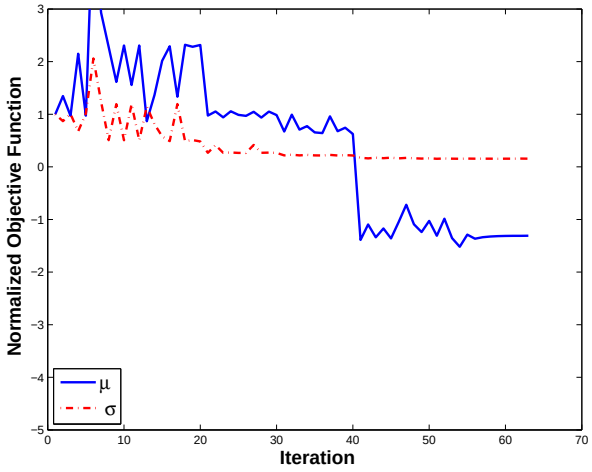

(c) Standard Dev. as Objective Function

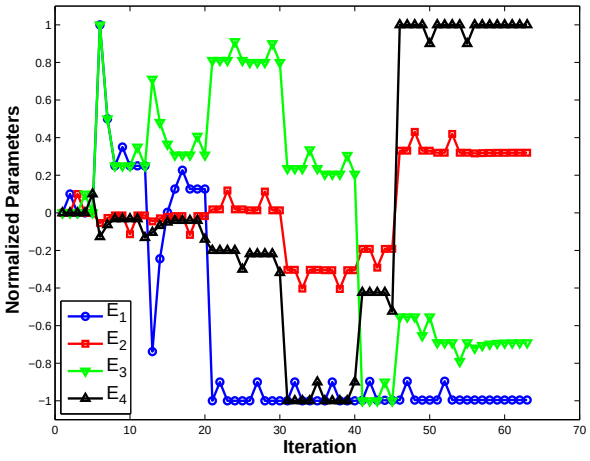

(d) Parameters Convergence

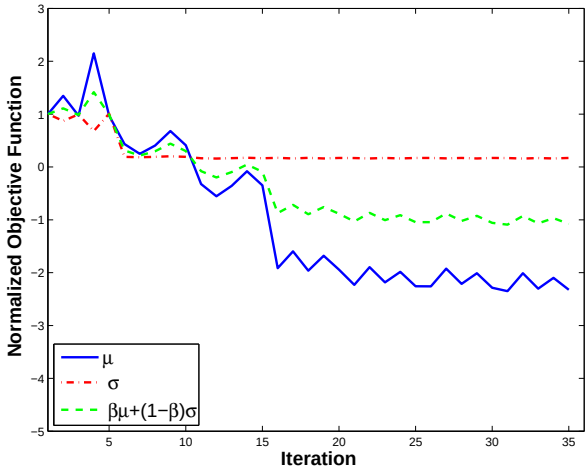

(e) Mean + Standard Dev. as Objective Function

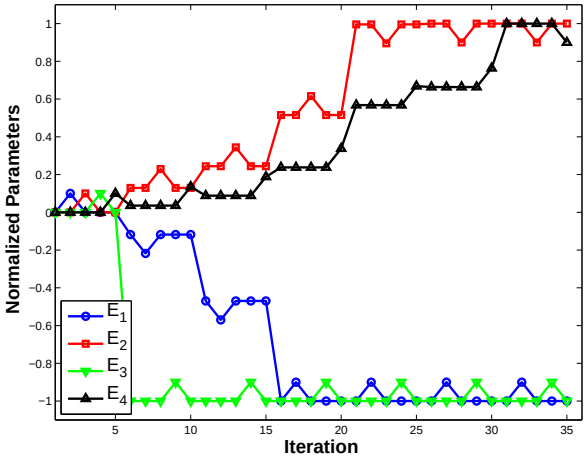

(f) Parameters Convergence

Figure 6. MDO Wing Optimization Convergence

VII. Conclusion & Outlook

The feasibility of performing robust flutter optimization in realistic wing structures in the transonic regime was investigated. By using modern aeroelastic stability analysis and uncertainty quantification techniques, such as the Schur Complement Method for Eigenvalue Analysis and NIPC, it was possible to optimize a wing structure taking into account tip mass and inertia variability. The wing tip's characteristics have a strong influence on aeroelastic behaviour, nevertheless it was possible to reduce the sensitivity of the wing to significant variations in tip mass properties, even considering only Young's modulus as a design variable. Future work should address what are the penalties in terms of structural weight of increasing the robustness and reliability of wing structures. This methodology is readily available to be used in such tasks and work is underway to address this issue.

References

[1]Janardhan, S. and Grandhi, R., "Multidisciplinary Optimization of an Aircraft Wing/Tip Store Configuration in the Transonic Regime," *Engineering Optimization*, Vol. 36, No. 4, 2004, pp. 473–490.

[2]Marques, S., Badcock, K., Khodaparast, H., and Mottershead, J., "Transonic Aeroelastic Stability Predictions Under the Influence of Structural Variability," *Journal of Aircraft*, Vol. 47, No. 4, 2010, pp. 1229–1239.

[3]Janardhan, S. and Grandhi, R., "Uncertainty Quantification in Aeroelasticity: Recent Results and Research Challenges," *Journal of Aircraft*, Vol. 41, No. 5, 2004, pp. 1217–1229.

[4]Badcock, K. and Woodgate, M., "Bifurcation Prediction of Large-Order Aeroelastic Models," *AIAA Journal*, Vol. 48, No. 6, 2010, pp. 1037–1046.

[5]Marques, S., Badcock, K., Khodaparast, H., and Mottershead, J., "On How Structural Model Variability Influences Transonic Aeroelastic Stability," *Journal of Aircraft*, in press.

[6]Marques, S. and Badcock, K., "Stochastic Optimization of Transonic Aeroelastic Structures," IFASD 2011-17, 2011, Presented at the Internatinoal Forum for Aeroelasticity and Structural Dynamics, Paris, France.

[7]Badcock, K., Woodgate, M., and Richards, "The Application of Sparse Matrix Techniques for the CFD based Aeroelastic Bifurcation Analysis of a Symmetric Aerofoil," *AIAA Journal*, Vol. 42, No. 5, 2004, pp. 883–892.

[8]Badcock, K., Woodgate, M., and Richards, "Direct Aeroelastic Bifurcation Analysis of a Symmetric Wing Based on the Euler Equations," *Journal of Aircraft*, Vol. 42, No. 3, 2005, pp. 731–737.

[9]Bekas, K. and Saad, Y., "Computation of Smallest Eigenvalues using Spectral Schur Complements," *SIAM Journal of Scientific Computing*, Vol. 27, No. 2, 2005, pp. 458–481.

[10]Manan, A. and Cooper, J., "Design of Composite Wings Including Uncertainties: A Probabilistic Approach," *Journal of Aircraft*, Vol. 46, No. 2, 2009, pp. 601–607, doi: 10.2514/1.39138.

[11]Allen, M. and Camberos, J., "Comparison of Uncertainty Propagation / Response Surface Techniques for Two Aeroelastic Systems," AIAA Paper 2009-2269, AIAA, 2009, Presented at the AIAA/ASME/ASCE/AHS/ASC Structures, Structural Dynamics, and Materials Conference, Palm Springs, California.

[12]Hosde, S., Walters, R., and Balch, M., "Point-Collocation Nonintrusive Polynomial Chaos Method for Stochastic Computational Fluid Dynamics," *AIAA Journal*, Vol. 48, No. 12, 2010, pp. 2721–2730, doi: 10.2514/1.39389.

[13]Park, G., Lee, T., Lee, K., and Hwang, K., "Robust Design: An Overview," *AIAA Journal*, Vol. 44, No. 1, 2006, pp. 181–191.

[14]Johnson, S. G., "The NLopt nonlinear-optimization package," April 2011.

[15]Powell, M. J. D., *Advances in Optimization and Numerical Analysis*, Kluwer Academic, 1994.

[16]Beran, P., Knot, N., Eastep, F., Synder, R., and Zweber, J., "Numerical Analysis of Store-Induced Limit Cycle Oscillarion," *Journal of Aircraft*, Vol. 41, No. 6, 2004, pp. 1315–1326.

[17]Girodroux-Lavigne, P., Grisval, J., Guillemot, S., Henshaw, M., Karlsson, A., Selmin, V., Smith, J., Teupootahiti, E., and Winzell, B.

[18]Allen, C., Jones, D., Taylor, N., Badcock, K., Woodgate, M., Rampurawala, A., Cooper, J., and Vio, G.